Design, synthesis, and evaluation of potent bryostatin analogs that modulate PKC translocation selectivity

Paul A. Wender[1], Jeremy L. Baryza, Stacey E. Brenner, Brian A. DeChristopher, Brian A. Loy, Adam J. Schrier, and Vishal A. Verma

Departments of Chemistry and of Chemical and Systems Biology, Stanford University, Stanford, CA 94305

Edited by Stuart L. Schreiber, Broad Institute, Cambridge, MA, and approved February 9, 2011 (received for review December 14, 2010)

Modern methods for the identification of therapeutic leads include chemical or virtual screening of compound libraries. Nature's library represents a vast and diverse source of leads, often exhibiting exquisite biological activities. However, the advancement of natural product leads into the clinic is often impeded by their scarcity, complexity, and nonoptimal properties or efficacy as well as the challenges associated with their synthesis or modification. Function-oriented synthesis represents a strategy to address these issues through the design of simpler and therefore synthetically more accessible analogs that incorporate the activity-determining features of the natural product leads. This study illustrates the application of this strategy to the design and synthesis of functional analogs of the bryostatin marine natural products. It is specifically directed at exploring the activity-determining role of bryostatin A-ring functionality on PKC affinity and selectivity. The resultant functional analogs, which were prepared by a flexible, modular synthetic strategy, exhibit excellent affinity to PKC and differential isoform selectivity. These and related studies provide the basic information needed for the design of simplified and thus synthetically more accessible functional analogs that target PKC isoforms, major targets of therapeutic interest.

Therapeutic leads are derived from or inspired by natural, nonnatural, and virtual sources. Nature's collection, a library representing 3.8 billion years of chemical evolution, is vast, structurally diverse, and remarkably rich with therapeutically promising molecules (1). This collection can also be readily expanded by harnessing the powerful capabilities of biosynthetic machinery using, for example, phage display (2), engineered biosynthesis (3–5), and synthetic biology. Complementing nature's library, fully synthetic libraries (6, 7) offer the notable advantage of being derivable from a more varied collection of bond construction methods, atoms, and building blocks than those used in nature. Virtual libraries (8, 9) provide a third and comprehensive source of lead structures and are limited only by bonding theory and self-imposed structure generation and selection criteria.

Although natural products have proven to be a very effective source of library leads, traditional medicines, and modern drugs (10), they are neither evolved nor optimized for human use. Furthermore, they are often scarce, too complex to synthesize in a practical fashion, or too difficult to derivatize as needed to optimize for therapeutic function. Function-oriented synthesis (FOS) offers a strategy to address these issues (11). FOS draws on the view that a specific function of a natural or nonnatural compound, whether it be a therapeutic, material, probe, nanodevice, imaging agent, diagnostic, catalyst, conductor, or a molecule of theoretical interest, can be achieved with many even simplified structures through synthesis-informed design. As it applies to therapeutic leads, FOS is based on the understanding that the activity (function) of a natural product is often determined by only a subset of its functionality and that such activity could thus be reproduced or improved by incorporating these function-determining features into simplified and therefore synthetically more accessible structures. The goal of FOS is to design for both optimal function and ease of synthesis, and an attractive aspect of this approach is that one can creatively select for desired structural, synthetic, pharmacokinetic, and activity goals. In essence, FOS focuses on function, the approach to which can be achieved through design, diversity-oriented synthesis, biology-oriented synthesis, diverted total synthesis, and others.

Our group has employed this approach in the design and development of numerous simplified agents that harness the functional activities of structurally complex natural leads. This strategy is also finding increasing success in other laboratories (12–16) and resonates in part with the goals and related concept of diverted total synthesis (17, 18). The starting point of FOS is function and the view that function could be emulated with a wide range of designed structures, as many structural types could mimic a natural product's shape and electron density features. This view draws validation from many sources including, for example, early studies on synthetic β-lactams. An early example of this FOS strategy in our own studies was the demonstration that the activity of the phorbol esters (29-step synthesis) could be emulated in part by highly simplified functional analogs available in only 7 steps (Fig. 1) (19). Bryostatin is another noteworthy example of this approach and forms the focus of this study.

The bryostatins are complex, scarce natural products produced by a bacterial symbiont (20, 21) of the marine bryozoan *Bugula neritina*. Extracts of this marine organism were reported to possess anticancer activities by Pettit et al. in 1970 (22), but it was not until 1982 that the structure of bryostatin 1 (Fig. 2), a primary active constituent of these extracts, was elucidated (23). Nineteen additional bryostatins have since been described.

The most thoroughly investigated member of this family is bryostatin 1, which possesses a remarkable if not unique portfolio of biological activities relevant to cancer therapy including modulation of apoptotic function (24), reversal of multidrug resistance (25, 26), and stimulation of the immune system (27). Bryostatin has been investigated for anticancer activity in over 35 phase I and II clinical trials (see http://clinicaltrials.gov). Its efficacy as a single agent has varied as a function of cancer type. More recently, studies have shown that it can enhance the clinical efficacy of known oncolytics in several cases (28–30). Additionally, bryostatin or its tunable analogs provide a starting point for promising immunotherapeutic approaches to cancer treatment (31). Notably, the required clinical dose of bryostatin is extraordinarily low (*ca.* 50 $\mu g/m^2$); only approximately 1 mg is needed for an eight-week clinical treatment cycle.

Of additional clinical significance, bryostatin enhances learning and extends memory in animal models (32, 33), which is attributable in part to its ability to induce synaptogenesis (34). These activities suggest that bryostatin or a more readily

Author contributions: P.A.W., J.L.B., S.E.B., B.A.D., B.A.L., A.J.S., and V.A.V. designed research; P.A.W., J.L.B., S.E.B., B.A.D., B.A.L., A.J.S., and V.A.V. analyzed data; J.L.B., S.E.B., B.A.D., B.A.L., A.J.S., and V.A.V. performed research; and P.A.W., B.A.L., A.J.S., and V.A.V. wrote the paper.

The authors declare no conflict of interest.

This article is a PNAS Direct Submission.

[1]To whom correspondence should be addressed. E-mail: wenderp@stanford.edu.

This article contains supporting information online at www.pnas.org/lookup/suppl/doi:10.1073/pnas.1015270108/-/DCSupplemental.

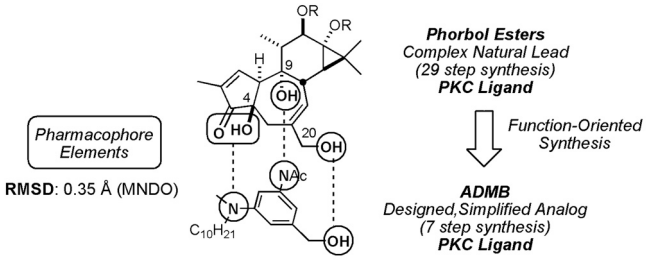

Fig. 1. The function-oriented synthetic approach to simplified analogs of the phorbol esters that possess affinity to PKC.

accessible designed analog (35) could serve as a first-in-class clinical lead for the treatment of Alzheimer's disease (36) and other neurodegenerative disorders (37). Bryostatin also exhibits neuroprotective capabilities in animal models of cerebral ischemia, indicating its potential use for minimizing the destructive neurological effects of stroke (38). Of special recent significance, bryostatin, not unlike prostratin (39), has been found to activate latent HIV reservoirs, providing a potential strategy for the eradication of HIV (40).

Notwithstanding its great therapeutic potential, research on and clinical development of bryostatin has been impeded by its low natural abundance. The GMP production of bryostatin for clinical use provided only 18 g of pure bryostatin 1 from *14 tons* of *B. neritina* (0.00014%) (41). Although this supply was sufficient to initiate preclinical and clinical research on bryostatin, economic and environmental factors have limited further development of this source. The yields of bryostatin's related congeners are similarly low (10^{-3} to 10^{-8}%) (42), and seasonal variability has further complicated isolation. Although chemical synthesis offers a supply possibility, published syntheses of the clinical lead or similarly potent congeners (K_i < 10 nM) have thus far been too long (>55 steps) to impact cost-effective supply (43–47). Similarly, engineered biosynthesis, although promising, is still in the early stages of development (48). A further consideration is that these strategies collectively provide only bryostatin or closely related derivatives, which are neither evolved nor optimized for human therapeutic use.

In 1986, our group set out to address both the supply *and* therapeutic optimization goals associated with bryostatin by using an FOS strategy. Bryostatin's activities are mediated by its interaction with several intracellular targets (49), including the diacylglycerol (DAG)-dependent isoforms of PKC, a family of kinases that transduce endogenous DAG and Ca^{2+} signals. DAG-dependent PKC is subdivided into two classes, conventional and novel (see *SI Appendix*) (50): Conventional PKCs (α, βI, βII, and γ) require both DAG and Ca^{2+}, whereas novel PKCs (δ, ϵ, θ, and η) are activated by DAG alone.

An initial goal of this program was to identify the functional groups in bryostatin that contribute to its activity. In collaboration with the groups of Pettit and Blumberg, we advanced the hypothesis based on structure–function analyses and computer structure comparisons that, of all possible pharmacophores in bryostatin, the C1-carbonyl, C19-OH, and C26-OH groups were compelling candidates for controlling its affinity to PKC (51). This hypothesis was supported by chemical derivatization studies, comparisons of natural product activities, and systematic structural comparison of bryostatin with structurally unrelated yet competitive PKC ligands (e.g., DAG and phorbol ester derivatives). This analysis suggested that bryostatin's southern or C-ring region directly contacts PKC and thus serves as its "recognition domain." It was additionally proposed (52) that the northern A- and B-ring regions serve as an important scaffolding element, or "spacer domain," that influences the presentation of bryostatin's pharmacophoric elements and possibly influences intracellular trafficking and membrane association.

This hypothesis led to the design of macrocycles containing bryostatin-like recognition domains but structurally simplified spacer domains (Fig. 2). In 1998, we reported an initial series of potent, fully synthetic bryologs that were prepared according to these design principles (53). We have since reported numerous potent, tunable bryologs exemplified by analog **1** (54). This compound possesses excellent affinity for PKC (K_i = 3 nM), is *orders of magnitude* more potent than bryostatin against several human cancer cell lines, and can be synthesized in a step-economical fashion (29 total steps) scalable to meet clinical demand. Recent work by Keck and coworkers has provided further examples of the effectiveness of this design strategy (55–58).

Step economy is enabled through design, both by simplification and careful scaffold engineering; substitution of the natural product's B-ring tetrahydropyran motif with a dioxane substructure allows for the mild, modular union of appropriately functionalized recognition and spacer domain elements by esterification followed by acid-promoted macrotransacetalization (Fig. 2). This dioxane for pyran substitution has also found value in other target simplifications (59). The modularity inherent to this convergent fragment coupling strategy renders it highly amenable to library synthesis. We have recently extended our convergent fragment coupling approach to the natural B-ring tetrahydropyran scaffold using a mechanistically related Prins macrocyclization reaction (60). To date, we have developed a library of over 100 bryologs,

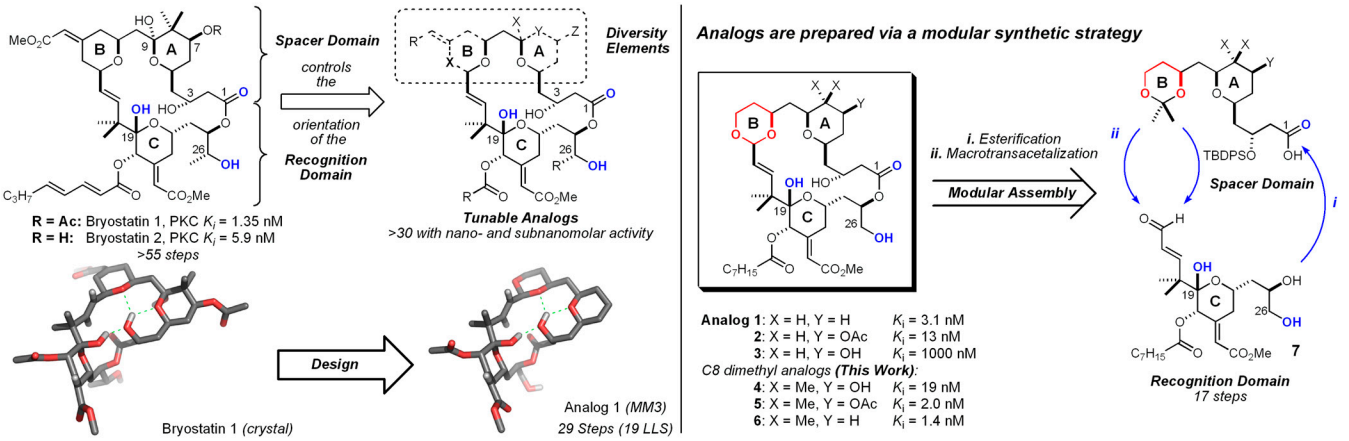

Fig. 2. (*Left*) Structures of bryostatin 1 and 2 and general analog design principle. Pharmacophoric atoms are in blue. Conformational depictions are derived from crystal structure (bryo 1) or Monte Carlo MM3 conformational search (analog 1). For clarity, C20 side chains are excluded (bryo) or were abbreviated for modeling efficiency (analog 1). (*Right*) General synthetic strategy for B-ring dioxane analogs. Analogs are modularly assembled via a late-stage esterification/macrotransacetalization coupling protocol.

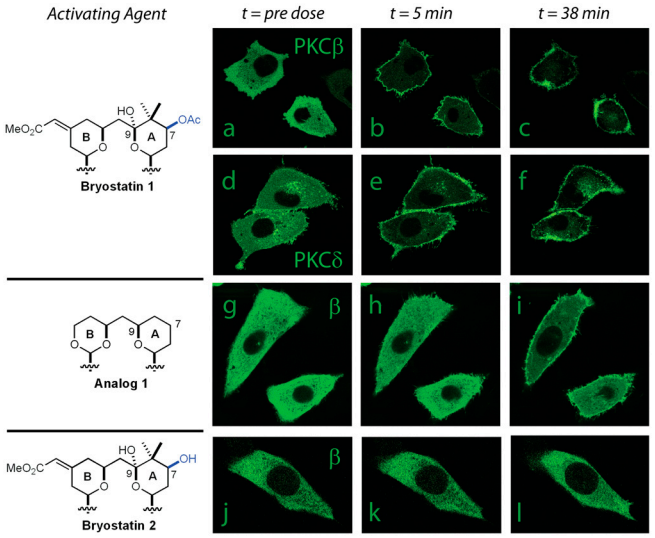

Fig. 3. (*A–C*) Translocation of PKCβ1-GFP by 200 nM bryostatin 1 in transiently transfected CHO-k1 cells, (*A*) Predose, (*B*) 5 min postdose, and (*C*) 38 min postdose. (*D–F*) Translocation of PKCδ-GFP by 200 nM bryo 1, same time points. (*G–I*) PKCβ1-GFP, 200 nM analog **1**, same time points. (*J–L*) PKCβ1-GFP, 200 nM bryostatin 2, same time points. See Fig. 6 *A* and *B* for quantification and time-course analysis.

more than 30 of which exhibit single-digit nanomolar or subnanomolar activities in PKC affinity or in vitro assays (61, 62). The most promising of these agents (e.g., **1**) are currently undergoing preclinical investigation for their use in cancer therapy (63), Alzheimer's disease (35), and latent HIV activation.

Because PKC plays a role in numerous biological processes ranging from apoptosis to cognition, an emerging goal of great importance is to understand whether analog affinity can be maintained while controlling functional isoform selectivity. Although PKC isoforms are in some cases functionally redundant, unique roles can be ascribed to each (64); thus, isotype selectivity is likely to be important in optimizing agents for desired functions while designing against unwanted activities or toxicities. Although some isoform- or class-selective PKC inhibitors have been developed (65, 66), they target the highly conserved ATP binding site of the human kinome. A promising complementary approach to isoform-selective PKC modulation is interference with, or simulation of, protein:protein interactions involved in the activation and localization of specific PKC isoforms (67). However, the general lack of selective modulators of the PKC C1 regulatory domain, for which gain and loss of function are possible, has slowed investigation of this signaling pathway and its clinical ramifications (68).

As described herein, the design, synthesis, and biological evaluation of systematically functionalized A-ring analogs **4–6** were investigated to better understand the relationship between A-ring functionality and PKC isoform selectivity. We find that the C8-geminal dimethyl unit incorporated into these analogs enhances their potency relative to des-methyl analogs **2** and **3**. Additionally, we find that the A-ring motif of these agents modulates their functional selectivity for representative PKC isoforms, providing a strong lead for development of more selective agents based on translocation kinetics.

Results and Discussion

Spacer Domain Structure Influences Conventional-PKC Activity. As a reference point for this study, we measured, using a previously described protocol (69, 70), the ability of natural bryostatins and synthetic analog **1** to translocate GFP fusion constructs of representative conventional and novel PKC isoforms in CHO-k1 cells. This assay relies on the mechanistic link between PKC activation and subcellular localization: Inactive PKC is located primarily in the cytosol and undergoes translocation to membranes when activated by bryostatin or other C1 domain modulators (50). The rate and extent of PKC activation induced by synthetic agents was measured in real time by changes in subcellular fluorescence intensity, and the localization of the activated kinase was directly observed. Additionally, preliminary isoform selectivity was investigated by comparing the relative activities of our agents for different PKC-GFP isoforms. For this study, we utilized PKCβ1-GFP and PKCδ-GFP as representative conventional and novel isoforms, respectively.

In accord with literature reports, bryostatin 1 was found to induce rapid translocation of PKCβ1 and PKCδ at a concentration of 200 nM (Fig. 3). The kinetics and extent of translocation are indistinguishable between isoforms, and activation is complete after several minutes following treatment. The dominant localization of both isoforms is the cellular membrane. Synthetic analog **1** at 200 nM possesses a similar ability to activate PKCδ as bryostatin 1; however, its ability to translocate PKCβ1 was attenuated relative to the natural product (Fig. 3, *G–I*). The activity of **1** at 2,000 nM was nearly indistinguishable from results obtained at 200 nM (see *SI Appendix*).

The differential translocation activities of bryostatin 1 and analog **1** for conventional PKC were also observed in NIH 3T3 mouse fibroblasts (71). In this system, the cellular localization of the conventional-PKCα isoform and novel isoforms PKCδ and ε was assessed via Western blot in response to incubation with 100 nM bryostatin 1 or analog **1**. Results are expressed as the ratio of cytosolic to membrane-bound PKC. Bryostatin 1 and analog **1** exhibit identical abilities to activate novel PKC isoforms in this system; complete membrane association of PKCδ and PKCε was observed after a 5-min incubation with either agent (Fig. 4 *A* and *B*). Mirroring the PKC-GFP observations, analog **1** exhibited a diminished ability to activate the conventional-PKCα isotype. Whereas bryostatin 1 induced complete membrane association of this isoform, analog **1** induced only $39 \pm 4\%$ translocation following a 30-min incubation. These selectivities were also observed for longer incubations; bryostatin 1 and analog **1** possess significantly ($\rho = 0.0057$) different abilities to down-regulate endogenous PKCα (Fig. 4 *C* and *D*), down-regulation being a phenomenon that typically follows prolonged PKC activation (50). After a 24-h incubation with 200 nM bryostatin 1, the majority of endogenous PKCα was degraded; however, $73 \pm 11\%$ of PKCα remained following similar exposure to analog **1**.

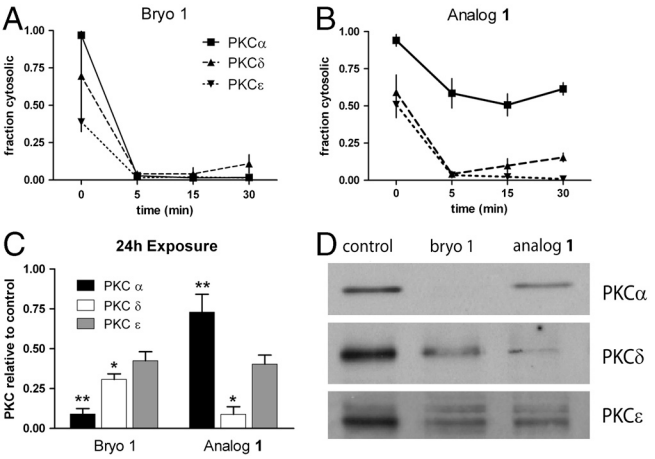

Fig. 4. (*A* and *B*) Band density analysis of endogenous PKC translocation in NIH 3T3 fibroblasts following incubation with 100-nM test compound. Results are an average of two to four experiments; error bars indicate SEM. (*C*) Endogenous PKC remaining relative to control in NIH 3T3 fibroblasts following a 24-h incubation with 200-nM test compound. (*D*) Representative experiment from 24-h degradation study.

As bryostatin 1 and analog **1** have similar PKC affinities, these combined results suggested that functional selectivity for novel PKC isoforms could be realized without sacrificing overall potency. Similar results have been observed for other synthetic analogs (72). Structurally, as the recognition domain elements of bryostatin 1 and analog **1** are very similar, we considered the possibility that the basis for these differential activities is contained in spacer domain functionality.

Pertinent to this hypothesis, we found that bryostatin 2, which is similarly potent (PKC $K_i = 5.9$ nM) to bryostatin 1 and differs structurally only by lack of a C7-acetate group, is unable to activate PKCβ1-GFP at 200 nM in CHO-k1 cells (Fig. 3). This finding implicated the A-ring region, particularly the C7 position, as a structural contributor to conventional-PKC activity and thus overall PKC selectivity.

Analog Design and Synthesis. For an initial investigation of the influence of C7 functionality on PKC selectivity, we recently prepared simplified C7-OAc and C7-OH bryologs **2** and **3** (Fig. 2) (73). Although C7-OAc analog **2** ($K_i = 13$ nM) has good affinity for PKC, C7-OH analog **3** ($K_i = 1{,}000$ nM) was found to be orders of magnitude less potent than bryostatin 2. As bryostatin 2 represents a significant lead in the development of novel isoform-selective PKC activators, we were prompted to determine what structural features might account for this potency difference. We reasoned that the C8-*gem* dimethyl moiety present in the natural product might mitigate the deleterious impact of its C7-OH moiety on potency. We therefore designed C8 *gem*-dimethyl bryologs **4**–**6** to test this hypothesis as well as to further probe the role of A-ring functionality on PKC affinity and selectivity. The C7-OAc and C7-OH analogs **4** and **5** were designed to probe the influence of C7 functionality on PKC selectivity, and the C7-deoxy analog **6** was prepared to parse out any individual contribution of the C8-*gem* dimethyl moiety.

We approached the syntheses of analogs **4**–**6** by way of common A-ring lactone **8** (Fig. 5), which was derived from *gem*-dimethyl ketone **9** and known aldehyde **10** (see *SI Appendix*). A diastereoselective aldol reaction between these partners preferentially gave hydroxyketone **11**. Although the 1,3-*anti* diastereoselectivity of this reaction was poor (1.5:1) using the lithium enolate of **9**, the cyclohexyl boron enolate gave an improved diastereomeric ratio (3:1). The *anti*:*syn* ratio was further improved to 9:1 by use of isopinocampheyl boron ligands. On a 5-g scale this process delivered hydroxyketone **11** in 64% isolated yield. Reduction with $Me_4NBH(OAc)_3$ (74) proceeded with exquisite *anti* selectivity to provide diol **12** in 85% yield after recrystallization. Acid-promoted lactonization differentiated the resulting diol motif to afford crystalline hydroxylactone **8**. This common intermediate was silylated for the synthesis of C7-oxy analogs **4** and **5**. Alternatively, deoxygenation gave lactone **14** in two steps and 91% yield en route to C7-deoxy analog **6**.

Lactones **13** and **14** both cleanly alkylated the dienolate of ethyl acetoacetate. The C9-lactol products were deoxygenated with TFA and Et_3SiH to give pyrans **15** and **16** in 50% and 51% yield over two steps, respectively. Noyori hydrogenation with [(R)-BINAP]$RuCl_2$ afforded the corresponding hydroxyesters with excellent diastereoselectivity (>95:5). These products were further reduced with $LiBH_4$ and protected as acetonides **17** and **18** in excellent overall yield. Debenzylation and oxidation provided the completed carboxylic acid spacer domain fragments **19** and **20**.

The highly convergent coupling of spacer domains **19** and **20** to previously described recognition domain **7** (54) was accomplished using Yamaguchi's esterification (Fig. 5*B*). Treatment of the resulting products with HF·pyridine effected, in one subsequent step, removal of all silyl protecting groups and macrotransacetalization to afford bryostatin 2-like C7-OH analog **4** and C7-deoxy analog **6** in 65% and 83% yield over two steps, respectively. Analog **4** was readily converted into bryostatin 1-like C7-OAc analog **5** in two steps and 88% yield by in situ silylation of C26 followed by acylation of C7 and subsequent desilylation.

Analog PKC Affinity and Selectivity. C8-*gem* dimethyl bryologs **4**, **5**, and **6** are potent ligands for a rat-brain PKC isozyme mixture (75), with K_i's of 19 nM, 2.0 nM, and 1.4 nM, respectively. When compared to *des*-methyl analogs **1**–**3**, the C8-dimethyl moiety enhances the PKC affinity of analogs bearing polar C7 functionality. C7-OAc analog **5** is 6.5-fold more potent than *des*-methyl analog **2** ($K_i = 13$ nM). More dramatically, C7-OH analog **4** is *50-fold* more potent than the *des*-methyl analog **3** ($K_i = 1{,}000$ nM). This affinity augmentation is less in the C7-deoxy series; the potencies of dimethyl analog **6** and analog **1** are quite similar. The origin of the large potency difference between **3** and **4** remains to be fully elucidated, but one possible explanation is that the sterically demanding C8-dimethyl moiety partially desolvates the neighboring C7-OH, diminishing penalties associated with protein binding and/or membrane association.

PKC-GFP translocation assays demonstrate that C7 modifications affect functional selectivity for PKC isoforms. As described above, the abilities of analogs to activate PKCδ-GFP

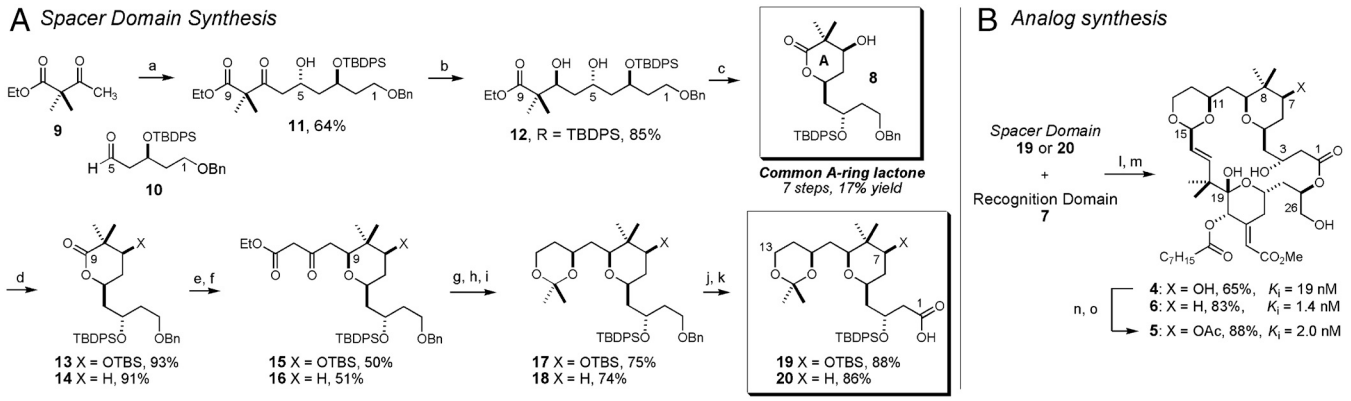

Fig. 5. (*A*) Synthesis of spacer domains for analog synthesis. Reagents and conditions: (a) Ketone **9**, (+)-Ipc$_2$BCl, Et_3N, Et_2O, 0 °C, then **10**, −98 °C, then H_2O_2, MeOH, pH 7 Buffer, 90:10 d.r., 64% isolated **11**; (b) $Me_4NBH(OAc)_3$, 1:1 HOAc:MeCN, −15 °C, 85% recrystallized yield; (c) (±)-CSA, PhH, reflux, 90% recrystallized yield; (d) when X = OTBS: TBS-OTf, 2,6-Lutidine, CH_2Cl_2; when X = H: (*i*) Im_2CS, CH_2Cl_2, (*ii*) Bu_3SnH, AIBN, $PhCH_3$, 110 °C; (e) ethyl acetoacetate, LDA, THF, −78 °C; (f) TFA, Et_3SiH, CH_2Cl_2; (g) Ru[(R)-BINAP]Cl_2 (2 mol%), EtOH, H_2 (78 bar), 35–40 °C; (h) $LiBH_4$, THF, (i) 2,2-dimethoxypropane, PPTS, DMF; (j) lithium naphthalenide, THF; (k) TEMPO (cat.), NaClO (cat.), $NaClO_2$, MeCN, pH 7 buffer. (*B*) Completion of bryologs **4**–**6**. Reagents and conditions: (l) 2,4,6-trichlorobenzoyl chloride, Et_3N, $PhCH_3$, then **7**, DMAP; (m) HF·pyridine, THF; (n) TESCl, DMAP, CH_2Cl_2, then Ac_2O; (o) HF·pyridine, THF.

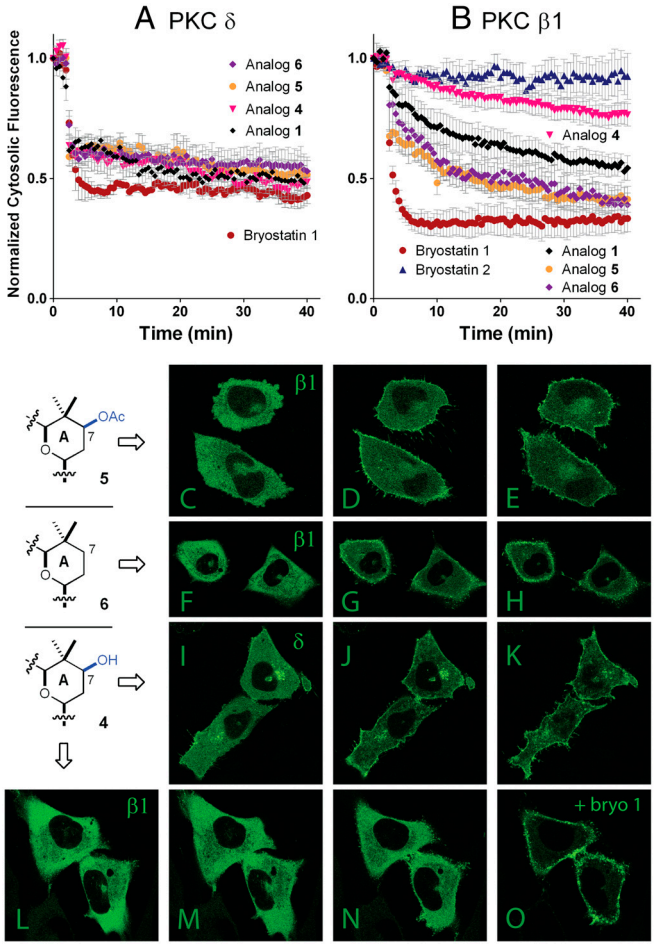

Fig. 6. (*A* and *B*) Normalized cytosolic fluorescence readings from translocation studies. Cells were dosed at 2.5 min. Decrease in cytosolic fluorescence indicates PKC activation. (*C–O*) Representative confocal images from cellular PKC-GFP translocation assays. (*C–E*, *F–H*, and *L–N*) Translocation of PKCβ1 by 200 nM **5**, **6**, or **4** at 0, 5, and 38 min postdose, respectively. (*I–K*) Translocation of PKCδ by 200 nM **4** at the same time points. (*O*) Translocation of PKCβ1 by 200 nM bryo 1 following initial treatment with 200 nM **4**.

and PKCβ1-GFP were measured in CHO-k1 cells. Analogs **4**, **5**, and **6** induced significant activation of novel PKCδ (Fig. 6*A*) at 200 nM. Translocation of fluorescence from the cytosol was immediately induced and was sustained over the 38-min observation period. The dominant localization of this isoform was the cellular membrane, although some intracellular compartmentalization was also observed (Fig. 6, *I–K*).

On the other hand, synthetic bryologs **4–6** differentially activated the conventional-PKCβ1 isoform. Most dramatically, in contrast to its ability to activate PKCδ, C7-OH analog **4** at a 200-nM concentration induced only minimal translocation of PKCβ1 (Fig. 6, *B* and *L–N*). Thus, at a therapeutically relevant concentration, analog **4** shows functional selectivity for the novel PKCδ isoform over the conventional-PKCβ1 isoform. Following incubation with **4**, translocation of PKCβ1 could be induced by administration of 200 nM of bryostatin 1 (Fig. 6*O*), indicating the presence of responsive kinase in these experiments.

In contrast, C7-OAc analog **5** and C7-deoxy analog **6** were able to activate PKCβ1 at 200 nM (Fig. 6, *B* and *C–H*); however, the activities of these agents were attenuated relative to bryostatin 1. The observed selectivities of these agents for novel PKCδ thus mimic that observed for analog **1**. As in the case of **1**, a 10-fold higher dose of **5** or **6** did not significantly enhance their PKCβ1 activity (see *SI Appendix*).

These combined observations indicate that the A ring of bryostatin and analogs modulates the activity of these agents for conventional PKC. We find that incorporation of a C8-*gem* dimethyl group is important for enhancing the PKC affinity of C7-OH analogs (e.g., analog **4**); this is significant as such compounds appear to have high functional selectivity for novel PKC isoforms. Intriguingly, synthetic analogs **1**, **5**, and **6** are capable of activating conventional-PKC although to a lesser extent than bryostatin 1. This difference contributes to bryostatin's ability to more effectively down-regulate the conventional-PKCα isozyme (Fig. 4). These and previous studies provide a collection of designed analogs covering a range of selectivities: Some members emulate bryostatin, whereas others exhibit complementary selectivities. Thus, the natural product and its synthetic analogs comprise a valuable set of tools to probe relationships between desired biological functions and selective modulation, activation, and down-regulation of the PKC family members.

Conclusions

The path of research progresses from information acquisition to understanding to the creative use of the resulting knowledge to produce solutions and products. Screening structures for sought-after function provides a point of entry along this path that is often required when structural leads are limited or absent. Natural products often provide a more advanced point of entry as activity (function) is often known. However, many are too scarce or complex to be synthesized and tuned for research or clinical advancement. As exemplified above, these problems can be addressed in part through an FOS strategy. In many cases, only a portion of a natural structure is needed for sought-after function. Knowledge of such structure–function dependencies can thus be used to design simpler compounds with comparable or superior activities that can be synthesized in a practical, step-economical fashion.

The above studies show that simplified bryostatin analogs can be prepared that have potencies comparable or superior to the natural product. Additionally, these agents exhibit PKC selectivities comparable or complementary to the natural product. The syntheses of these analogs are up to 25 steps shorter than published syntheses of the highly potent natural product congeners. Although this gap will no doubt decrease as more step-economical syntheses of bryostatins are reported, access to the simplified analogs will also improve. Given the comparable potency of bryostatin and the bryologs, the synthetic route to lead analog **1** involving 29 steps could now be used to supply clinical studies. Importantly, these studies allow rapid access to designed, tunable analogs and the opportunity to investigate their rich chemical biology, selectivity in target activation, and therapeutic potential as related to cancer, Alzheimer's disease, and HIV eradication.

Materials and Methods

Synthetic procedures and compound characterization data for all previously undescribed compounds, along with experimental protocols for PKC affinity, activation, translocation, and degradation assays, can be found in *SI Appendix*.

ACKNOWLEDGMENTS. We thank Professor Tobias Meyer (Stanford University, Stanford, CA) for the generous gift of PKC-GFP DNA plasmids and Professors Daria Mochly-Rosen and Lynette Cegelski for support with biological materials and equipment. Support of this work through a grant (CA31845) provided by the National Institutes of Health is gratefully acknowledged.

1. Wender PA, Miller BL (2009) Synthesis at the molecular frontier. *Nature* 460:197–201.
2. Smith GP, Petrenko VA (1997) Phage display. *Chem Rev* 97:391–410.
3. Tsoi CJ, Khosla C (1995) Combinatorial biosynthesis of 'unnatural' natural products: The polyketide example. *Chem Biol* 2:355–362.
4. Pfeifer BA, Admiraal SJ, Gramajo H, Cane DE, Khosla C (2001) Biosynthesis of complex polyketides in a metabolically engineered strain of *E. coli*. *Science* 291:1790–1792.
5. Menzella HG, et al. (2005) Combinatorial polyketide biosynthesis by de novo design and rearrangement of modular polyketide synthase genes. *Nat Biotechnol* 23:1171–1176.

6. Schreiber SL (2000) Target-oriented and diversity-oriented organic synthesis in drug discovery. *Science* 287:1964–1969.
7. Cordier C, Morton D, Murrison S, Nelson A, O'Leary-Steele C (2008) Natural products as an inspiration in the diversity-oriented synthesis of bioactive compound libraries. *Nat Prod Rep* 25:719–737.
8. Kolb P, Ferreira RS, Irwin JJ, Shoichet BK (2009) Docking and chemoinformatic screens for new ligands and targets. *Curr Opin Biotechnol* 20:429–436.
9. Reymond JL, van Deursen R, Blum LC, Ruddigkeit L (2010) Chemical space as a source for new drugs. *MedChemComm* 1:30–38.
10. Newman DJ, Cragg GM (2007) Natural products as sources of new drugs over the last 25 years. *J Nat Prod* 70:461–477.
11. Wender PA, Verma VA, Paxton TJ, Pillow TH (2008) Function-oriented synthesis, step economy, and drug design. *Acc Chem Res* 41:40–49.
12. Ii K, Ichikawa S, Al-Dabbagh B, Bouhss A, Matsuda A (2010) Function-oriented synthesis of simplified caprazamycins: discovery of oxazolidine-containing uridine derivatives as antibacterial agents against drug-resistant bacteria. *J Med Chem* 53:3793–3813.
13. Velvadapu V, et al. (2010) Desmethyl macrolides: Synthesis and evaluation of 4,8, 10-tridesmethyl telithromycin. *ACS Med Chem Lett* 2:68–72.
14. Gloeckner C, et al. (2010) Repositioning of an existing drug for the neglected tropical disease Onchocerciasis. *Proc Natl Acad Sci USA* 107:3424–3429.
15. Rizvi SA, et al. (2010) Rationally simplified bistramide analog reversibly targets actin polymerization and inhibits cancer progression *in vitro* and *in vivo*. *J Am Chem Soc* 132:7288–7290.
16. Dandapani S, Marcaurelle LA (2010) Current strategies for diversity-oriented synthesis. *Curr Opin Chem Biol* 14:362–370.
17. Wilson RW, Danishefsky SJ (2006) Small molecule natural products in the discovery of therapeutic agents: The synthesis connection. *J Org Chem* 71:8329–8351.
18. Szpilman AM, Carreira EM (2010) Probing the biology of natural products: Molecular editing by diverted total synthesis. *Angew Chem Int Ed* 49:9592–9628.
19. Wender PA, Koehler KF, Sharkey NA, Dell'Aquila ML, Blumberg PM (1986) Analysis of the phorbol ester pharmacophore on protein kinase C as a guide to the rational design of new classes of analogs. *Proc Natl Acad Sci USA* 83:4214–4218.
20. Davidson SK, Allen SW, Lim GE, Anderson GM, Haygood MG (2001) Evidence for the biosynthesis of bryostatins by the bacterial symbiont "*Candidatus* Endobugula sertula" of the Bryozoan *Bugula neritina*. *Appl Environ Microbiol* 67:4531–4537.
21. Lopanik N, Lindquist N, Targett N (2004) Potent cytotoxins produced by a microbial symbiont protect host larvae from predation. *Oecologia* 139:131–139.
22. Pettit GR, Day JF, Hartwell JL, Wood HB (1970) Antineoplastic components of marine animals. *Nature* 227:962–963.
23. Pettit GR, et al. (1982) Isolation and structure of bryostatin 1. *J Am Chem Soc* 104:6846–6848.
24. Wall NR, Mohammad RM, Al-Katib AM (1999) Bax:Bcl-2 ratio modulation by bryostatin 1 and novel antitubulin agents is important for susceptibility to drug induced apoptosis in the human early pre-B acute lymphoblastic leukemia cell line, Reh. *Leuk Res* 23:881–888.
25. Spitaler M, Utz I, Hilbe W, Hofmann J, Grunicke HH (1998) PKC-independent modulation of multidrug resistance in cells with mutant (V185) but not wild-type (G185) p-glycoprotein by bryostatin 1. *Biochem Pharmacol* 56:861–869.
26. Elgie AW, et al. (1998) Modulation of resistance to ara-C by bryostatin in fresh blast cells from patients with AML. *Leuk Res* 22:373–378.
27. Oz HS, Hughes WT, Rehg JE, Thomas EK (2000) Effect of CD40 ligand and other immunomodulators on Pneumocystis carinii infection in rat model. *Microb Pathog* 29:187–190.
28. Dowlati A, et al. (2003) Phase I and correlative study of combination bryostatin 1 and vincristine in relapsed B-cell malignancies. *Clin Cancer Res* 9:5929–5935.
29. Barr PM, et al. (2009) Phase II study of bryostatin 1 and vincristine for aggressive non-Hodgkin lymphoma relapsing after an autologous stem cell transplant. *Am J Hematol* 84:484–487.
30. Ajani JA, et al. (2006) A multi-center phase II study of sequential paclitaxel and bryostatin-1 (NSC 339555) in patients with untreated, advanced gastric or gastroesophageal junction adenocarcinoma. *Invest New Drugs* 24:353–357.
31. Shaha SP, et al. (2009) Prolonging microtubule dysruption enhances the immunogenicity of chronic lymphocytic leukaemia cells. *Clin Exp Immunol* 158:186–198.
32. Sun MK, Alkon DL (2005) Dual effects of bryostatin-1 on spatial memory and depression. *Eur J Pharm* 512:43–51.
33. Kuzirian AM, et al. (2006) Bryostatin enhancement of memory in Hermissenda. *Biol Bull* 210:201–214.
34. Hongpaisan J, Alkon DL (2007) A structural basis for enhancement of long-term associative memory in single dendritic spines regulated by PKC. *Proc Natl Acad Sci USA* 104:19571–19576.
35. Khan TK, Nelson TJ, Verma VA, Wender PA, Alkon DL (2009) A cellular model of Alzheimer's disease therapeutic efficacy: PKC activation reverses Aβ-induced biomarker abnormality on cultured fibroblasts. *Neurobiol Dis* 34:332–339.
36. Etcheberrigaray R, et al. (2004) Therapeutic effects of PKC activators in Alzheimer's disease transgenic mice. *Proc Natl Acad Sci USA* 101:11141–11146.
37. Sun MK, Alkon DL (2006) Bryostatin-1: Pharmacology and therapeutic potential as a CNS drug. *CNS Drug Rev* 12:1–8.
38. Sun MK, Hongpaisan J, Alkon DL (2009) Postischemic PKC activation rescues retrograde and anterograde long-term memory. *Proc Natl Acad Sci USA* 106:14676–14680.
39. Wender PA, Kee J-M, Warrington JM (2008) Practical synthesis of prostratin DPP and their analogs, adjuvant leads against latent HIV. *Science* 320:649–652.
40. Mehla R, et al. (2010) Bryostatin modulates latent HIV-1 infection via PKC and AMPK signaling but inhibits acute infection in a receptor independent manner. *PLoS One* 5: e11160.
41. Schaufelberger DE, et al. (1991) The large-scale isolation of bryostatin 1 from *Bugula neritina* following current good manufacturing practices. *J Nat Prod* 54:1265–1270.
42. Pettit GR (1996) Progress in the discovery of biosynthetic anticancer drugs. *J Nat Prod* 59:812–821.
43. Kageyama M, et al. (1990) Synthesis of bryostatin 7. *J Am Chem Soc* 112:7407–7408.
44. Evans DA, et al. (1999) Total synthesis of bryostatin 2. *J Am Chem Soc* 121:7540–7552.
45. Ohmori K, et al. (2000) Total synthesis of bryostatin 3. *Angew Chem Int Ed* 39:2290–2294.
46. Trost BM, Dong G (2008) Total synthesis of bryostatin 16 using atom-economical and chemoselective approaches. *Nature* 456:485–488.
47. Keck GE, Poudel YB, Cummins TJ, Rudra A, Covel JA (2011) Total synthesis of bryostatin 1. *J Am Chem Soc* 133:744–747.
48. Trindade-Silva AE, Lim-Fong GE, Sharp KH, Haygood MG (2010) Bryostatins: Biological context and biotechnological prospects. *Curr Opin Biotechnol* 21:834–842.
49. Kazanietz MG (2002) Novel "nonkinase" phorbol ester receptors: The C1 domain connection. *Mol Pharmacol* 61:759–767.
50. Newton AC (2001) Protein kinase C: structural and spatial regulation by phosphorylation, cofactors, and macromolecular interactions. *Chem Rev* 101:2353–2364.
51. Wender PA, et al. (1988) Modeling of the bryostatins to the phorbol ester pharmacophore on protein kinase C. *Proc Natl Acad Sci USA* 85:7197–7201.
52. Wender PA, et al. (1998) The design, computer modeling, solution structure, and biological evaluation of synthetic analogs of bryostatin 1. *Proc Natl Acad Sci USA* 95:6625–6629.
53. Wender PA, et al. (1998) Synthesis of the first members of a new class of biologically active bryostatin analogs. *J Am Chem Soc* 120:4534–4535.
54. Wender PA, et al. (2002) The practical synthesis of a novel and highly potent analogue of bryostatin. *J Am Chem Soc* 124:13648–13649.
55. Keck GE, et al. (2008) Convergent assembly of highly potent analogues of bryostatin 1 via pyran annulation: Bryostatin look-alikes that mimic phorbol ester function. *J Am Chem Soc* 130:6660–6661.
56. Keck GE, et al. (2009) Substitution on the A-ring confers to bryopyran analogues the unique biological activity characteristics of bryostatins and distinct from that of the phorbol esters. *Org Lett* 11:593–596.
57. Keck GE, et al. (2009) The bryostatin 1 A-ring acetate is not the critical determinant for antagonism of phorbol ester-induced biological responses. *Org Lett* 11:2277–2280.
58. Keck GE, et al. (2010) Molecular modeling, total synthesis, and biological evaluations of C9-deoxy bryostatin 1. *Angew Chem Int Ed* 49:4580–4584.
59. Smith AB, Razler TM, Meis RM, Pettit GR (2006) Design and synthesis of a potent phorboxazole C(11–15) acetal analogue. *Org Lett* 8:797–799.
60. Wender PA, DeChristopher BA, Schrier AJ (2008) Efficient synthetic access to a new family of highly potent bryostatin analogues via a Prins-driven macrocyclization strategy. *J Am Chem Soc* 130:6658–6659.
61. Wender PA, Hinkle KW, Koehler MFT, Lippa B (1999) The rational design of potential chemotherapeutic agents: Synthesis of bryostatin analogues. *Med Res Rev* 19:388–407.
62. Wender PA, et al. (2007) Beyond natural products: Synthetic analogs of bryostatin 1. *Drug Discovery Research: New Frontiers in the Post-Genomic Era*, ed Z Huang (Wiley-VCH, Hoboken, NJ), pp 127–162.
63. Stang SL, et al. (2009) A proapoptotic signaling pathway involving RasGRP, Erk, and Bim in B cells. *Exp Hematol* 37:122–134.
64. Griner EM, Kazanietz MG (2007) Protein kinase C and other diacylglycerol effectors in cancer. *Nat Rev Cancer* 7:281–294.
65. Ishii H, et al. (1996) Amelioration of vascular dysfunctions in diabetic rats by an oral PKC β inhibitor. *Science* 272:728–731.
66. Martiny-Baron G, et al. (1993) Selective inhibition of protein kinase C isozymes by the indolocarbazole Gö 6976. *J Biol Chem* 268:9194–9197.
67. Churchill EN, Kvit N, Mochly-Rosen D (2009) Rationally designed peptide regulators of protein kinase C. *Trends Endocrinol Metab* 20:25–33.
68. Mackay HJ, Twelves CJ (2007) Targeting the protein kinase C family: Are we there yet? *Nat Rev Cancer* 7:554–562.
69. Oancea E, Meyer T (1998) Protein kinase C as a molecular machine for decoding calcium and diacylglycerol signals. *Cell* 95:307–318.
70. Baryza JL, Brenner SE, Craske ML, Meyer T, Wender PA (2004) Simplified analogs of bryostatin with anticancer activity display greater potency for translocation of PKCδ-GFP. *Chem Biol* 11:1261–1267.
71. Szallasi Z, Smith CB, Pettit GR, Blumberg PM (1994) Differential regulation of protein kinase C isozymes by bryostatin 1 and phorbol 12-myristate 13-acetate in NIH 3T3 fibroblasts. *J Biol Chem* 269:2118–2124.
72. Wender PA, Verma VA (2006) Design, synthesis, and biological evaluation of a potent PKC selective, B-ring analog of bryostatin. *Org Lett* 8:1893–1896.
73. Wender PA, Verma VA (2008) The design, synthesis, and evaluation of C7 diversified bryostatin analogs reveals a hot spot for PKC affinity. *Org Lett* 10:3331–3334.
74. Evans DA, Chapman KT, Carreira EM (1988) Directed reduction of β-hydroxy ketones employing tetramethylammonium triacetoxyborohydride. *J Am Chem Soc* 110:3560–3578.
75. Mochly-Rosen D, Koshland DE, Jr (1987) Domain structure and phosphorylation of protein kinase C. *J Biol Chem* 262:2291–2297.